Global performance metrics for synchronization of heterogeneously rated power systems: The role of machine models and inertia

Fernando Paganini, *Fellow, IEEE*, and Enrique Mallada, *Member, IEEE*

Abstract— **A recent trend in control of power systems has sought to quantify the synchronization dynamics in terms of a global performance metric, compute it under very simplified assumptions, and use it to gain insight on the role of system parameters, in particular, inertia. In this paper, we wish to extend this approach to more realistic scenarios, by incorporating the heterogeneity of machine ratings, more complete machine models, and also to more closely map it to classical power engineering notions such as Nadir, Rate of Change of Frequency (RoCoF), and inter-area oscillations.**

We consider the system response to a step change in power excitation, and define the system frequency as a weighted average of generator frequencies (with weights proportional to each machine's rating); we characterize Nadir and RoCoF by the L_∞ norm of the system frequency and its derivative, respectively, and inter-areas oscillations by the L_2 norm of the error of the vector of bus frequencies w.r.t. the system frequency.

For machine models where the dynamic parameters (inertia, damping, etc.) are proportional to rating, we analytically compute these norms and use them to show that the role of inertia is more nuanced than in the conventional wisdom. With the classical swing dynamics, inertia constant plays a secondary role in performance. It is only when the turbine dynamics are introduced that the benefits of inertia become more prominent.

I. Introduction

The synchronization performance of the power grid has been a major concern of system operators since the early days [1], [2]. Most generators and loads are designed on the assumption that the grid frequency is tightly regulated around a nominal value (e.g. 60Hz in the U.S., 50Hz in Europe). When the frequency deviates significantly (a few hundred mHz) due to some network fault, several mechanisms, such as machine protections or under frequency load shedding (ULFS) [3], automatically disconnect critical network elements, potentially causing cascading failures and ultimately blackouts [4].

The gradual substitution of conventional electromechanical with renewable generation has raised new concerns about synchronization performance. The former provide a natural response to power imbalances, which is not present in the inverter-based interfaces of renewable sources; in particular the lack of *inertia* in the latter is often seen as a threat to frequency regulation. An objective analysis of this issue requires identifying appropriate performance *metrics*.

Two separate mechanisms are at play in frequency fluctuations. On one hand, abrupt changes on the global

supply-demand balance induce system-wide frequency changes, which may persist in steady state. On the other hand, geographically-distributed frequency oscillations (a.k.a. inter-area oscillations) [5], [6], [7] may be observed due to weak global coupling. Good performance metrics should be able to identify and discriminate between these two phenomena.

To address these problems, power engineers have traditionally relied on classical control metrics. For example, they use the system response to a step input to measure the maximum frequency deviation to imbalances (Nadir) as well as the maximum rate of change of frequency (RoCoF)[8]; their main limitation is that these quantities are node dependent. To evaluate inter-area oscillations, eigenvalue methods (slow coherency [9], participation factors [10]) have been employed.

More recently, a trend in control of power systems has aimed to quantify synchronization performance in terms of *global* system metrics such as $\mathcal{H}_2$ or $\mathcal{H}_\infty$ [11], [12], [13], [14], [15], [16], [17]. These norms capture the effect of system parameters, such as inertia, damping, and the eigenvalues of the network (Laplacian) matrix, on system performance. However, closed-form analytic results depend on oversimplified assumptions –homogeneous machines modeled by swing equations– and do not directly represent step-response information which is most important for network operators to analyze disturbances.

In this paper, we wish to bridge the gap between the two approaches. Firstly, to extend the latter approach to cover more realistic scenarios by incorporating heterogeneity of machine ratings, and adding turbine dynamics. Secondly, to incorporate step-response metrics (Nadir, RoCoF) for an appropriately defined global system frequency, and to separately characterize inter-area oscillations.

To obtain analytically tractable results, we focus on a specifically family of heterogeneous machines, in which key dynamic parameters are proportional to rating. This restriction is mild in comparison with homogeneity, and enables a diagonalization procedure, generalizing traditional eigen-analysis. From it, a *system frequency* suitable for step response analysis appears naturally, and turns out to be

$$\bar{w}(t) := \frac{\sum_i m_i w_i}{\sum_i m_i}, \tag{1}$$

the weighted average of node frequencies in proportion to their inertia. This is identical to the frequency of the center of inertia (COI) a classical notion [18], [19]. Nadir and RoCoF are defined as the $\mathcal{L}_\infty$ norms of, respectively, $\bar{w}(t)$

and $\dot{\bar{w}}(t)$. A synchronization cost measuring transient inter-area oscillations is defined as the $\mathcal{L}_2$ norm of the vector of deviations $\tilde{w}_i(t) = w_i(t) - \bar{w}(t)$.

The rest of the paper is organized as follows. In Section II we formulate the model and carry out the diagonalization of the dynamics, making the above decomposition precise. The system frequency step response, and a closed form expression for the synchronization cost, are both expressed in terms of a representative machine and the network structure.

In Sections III and IV we apply the results to different machine models, respectively to the second-order swing dynamics, and a third-order model that incorporates the turbine control. We find that some important aspects, in particular the importance of inertia, depend crucially on the chosen model. The paper concludes with a discussion in Section V, and some derivations are covered in the Appendix.
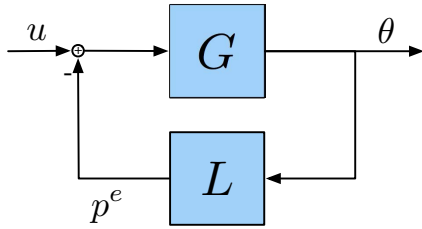
II. DYNAMIC MODEL WITH MACHINE HETEROGENEITY

Fig. 1.   Block Diagram of Linearized Power Network

We consider a set of n generator buses, indexed by i, dynamically coupled through an AC network. Assuming operation around an equilibrium, the linearized dynamics are represented by the block diagram in Fig. 1, where:

- $G(s) = \mathrm{diag}(g_i(s))$ is the diagonal transfer function of generators at each bus. Each $g_i(s)$ has as output the phase angle θ_i, and as input the net power at its generator axis, relative to its equilibrium value. This includes an outside disturbance u_i, reflecting variations in mechanical power or local load, minus the variation p_i^e in electrical power drawn from the network.
- Using a linear DC model for the network, the vector of drawn power is written as $p^e = L\theta$, where L is the weighted Laplacian of the graph defined by the line susceptances. Thus all the coupling between the bus subsystems is through this feedback term. L is a rank $n-1$ matrix with kernel spanned by $\mathbf{1}$, the vector of all ones.

Two examples of generator dynamics, to be considered explicitly in this paper, are:

Example 1: The swing equation dynamics

$$\dot{\theta}_i = w_i,$$
$$m_i \dot{w}_i = -d_i w_i + u_i - p_i^e.$$

This corresponds to the transfer function

$$g_i(s) = \frac{1}{m_i s^2 + d_i s}. \qquad (2)$$

Example 2: The swing equation with a first-order model of the turbine control:

$$\dot{\theta}_i = w_i,$$
$$m_i \dot{w}_i = -d_i w_i + q_i + u_i - p_i^e,$$
$$\tau_i \dot{q}_i = -r_i^{-1}\omega - q_i.$$

Here q_i is the (variation of) turbine power, τ_i the turbine time constant and r_i the droop coefficient; the governor dynamics are considered to be faster and neglected. The corresponding transfer function is

$$g_i(s) = \frac{\tau_i s + 1}{s\left(m_i \tau_i s^2 + (m_i + d_i \tau_i)s + d_i + r_i^{-1}\right)}. \qquad (3)$$

Of course, other models are possible within this framework (e.g. a 4th order system including a state for the governors).

A. A family of heterogeneous machines

A popular research topic in recent years [11], [12], [13], [14], [15], [16], [17] has been the application of global metrics from robust control to this kind of synchronization dynamics, as a tool to shed light on the role of various parameters, e.g. system inertia. Most of the analytical results, however, consider a *homogeneous* network where all machines are identical (i.e., common m_i, d_i, etc.), a very restrictive scenario.[1]

In a real network, where generators have different power ratings, it is natural for parameters to scale accordingly: for instance, the inertia m_i of a machine will grow with its rating, and it is clear that "heavier" machines will have a more significant impact in the overall dynamics.

While in principle one would like to cover general parameters, we show here that a compact analysis can be given for the case where parameters satisfy a certain proportionality. We formalize this by introducing a *rating parameter* $0 < f_i \le 1$, defined in relation to the largest machine which has $f_i = 1$, and imposing the following:

Assumption 1: There exists a fixed transfer function $g_0(s)$, termed the *representative machine*, such that

$$g_i(s) = \frac{1}{f_i} g_0(s)$$

for each i, where $f_i > 0$ is the rating parameter of bus i.

To interpret this, consider first the swing dynamics of Example 1. Then the assumption is satisfied provided that inertia and damping are both proportional[2] to f_i, i.e. $m_i = f_i m$, $d_i = f_i d$, where m, d are those of the largest (representative) machine,

$$g_0(s) = \frac{1}{ms^2 + ds}.$$

Going to the case of Example 2 with the turbine dynamics, we find that the above assumption is satisfied provided that $m_i = f_i m$, $d_i = f_i d$, $r_i^{-1} = f_i r^{-1}$, $\tau_i = \tau$; here the inverse droop coefficient is assumed proportional to rating, but the turbine time-constant is taken to be homogeneous.

---

[1]Some bounds on heterogenous systems are given in [11], [14]. Numerical studies with heterogeneity are given in [12].

[2]This kind of proportionality is termed "uniform damping" in [19].

The corresponding representative machine is

$$g_0(s) = \frac{\tau s + 1}{s\left(m\tau s^2 + (m + d\tau)s + d + r^{-1}\right)}.$$

Regarding the practical relevance of our simplifying assumption: empirical values reported in [20] indicate that at least in regard to orders of magnitude, proportionality is a reasonable first-cut approximation to heterogeneity, substantially more realistic than the homogeneous counterpart.

B. Diagonalization

We will now exploit the above assumption to transform the dynamics of Fig. 1 in a manner that allows for a suitable decoupling in the analysis. In what follows, $F = \mathrm{diag}(f_i)$ denotes the diagonal matrix of rating parameters. Writing

$$G(s) = \mathrm{diag}(g_i(s)) = F^{-\frac{1}{2}}[g_0(s)I]F^{-\frac{1}{2}},$$

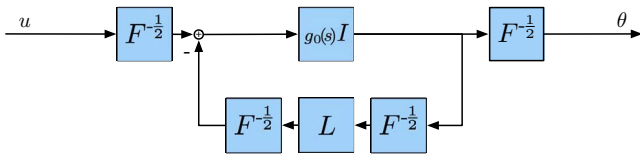we transform the feedback loop into the equivalent form of Fig. 2.

Fig. 2. Equivalent block diagram for heterogeneously rated machines

We introduce a notation for the scaled Laplacian matrix[3]

$$L_F := F^{-\frac{1}{2}}LF^{-\frac{1}{2}}, \tag{4}$$

which is positive semidefinite and of rank $n - 1$. Applying the spectral theorem we diagonalize it as

$$L_F = V\Lambda V^T, \tag{5}$$

where $\Lambda = \mathrm{diag}(\lambda_k)$, $0 = \lambda_0 < \lambda_1 \leq \cdots \leq \lambda_{n-1}$, and V is unitary. Distinguishing the eigenvector v_0 that corresponds to the zero eigenvalue, we write $V = [v_0 \quad V_\perp]$, where

$$V_\perp \in \mathbb{R}^{n \times (n-1)}, \ V_\perp^T V_\perp = I_{n-1}, \ V_\perp^T v_0 = 0.$$

In fact v_0 can be made explicit by recalling that $\ker(L) = \mathrm{span}\{\mathbf{1}\}$, so $\ker(L_F) = \mathrm{span}\{F^{\frac{1}{2}}\mathbf{1}\}$, from where

$$v_0 = \alpha_F F^{\frac{1}{2}}\mathbf{1}, \quad \text{with } \alpha_F := \left(\sum_i f_i\right)^{-\frac{1}{2}}. \tag{6}$$

Substitution of (5) into Fig. 2 and some block manipulations leads to the equivalent representation of Fig. 3.

Noting finally that the V block commutes with $g_0(s)I$ and thus cancels out with V^T, the internal loop is now fully diagonalized, yielding the closed-loop transfer function

$$H(s) = \mathrm{diag}(h_k(s)), \quad \text{with}$$

$$h_k(s) = \frac{g_0(s)}{1 + \lambda_k g_0(s)}, \quad k = 0, 1, \ldots, n - 1. \tag{7}$$

[3]This scaling already appears in the classical paper [9].
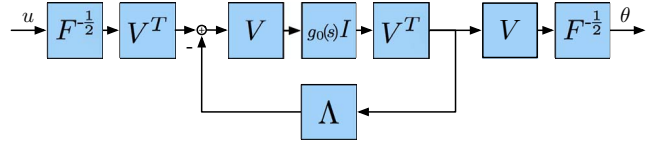

Fig. 3. Equivalent block diagram for heterogeneously rated machines with diagonalized closed loop

Assumption 2: The proportional feedback $\lambda_k > 0, k = 1, \ldots, n - 1$ is stabilizing for $g_0(s)$, i.e. $h_k(s)$ has all its poles in $Re[s] < 0$ for $k = 1, \ldots, n - 1$.

Later on we will verify that the assumption always holds for the two examples considered.

As for $h_0(s)$, we see that here there is no feedback: $h_0(s) = g_0(s)$. In the examples above, $g_0(s)$ has a pole at $s = 0$, which corresponds to the integration from frequency to angle. This is the typical situation in which the *local* control of the machine has no angle feedback, the latter only appears when considering coupling through the network.

Returning to Fig. 3 we arrive at the transfer function

$$T_{\theta u}(s) = F^{-\frac{1}{2}}VH(s)V^T F^{-\frac{1}{2}}$$

between the vector of external power disturbances and the machine angle outputs. If the output of interest is chosen to be the vector of frequencies, the relevant transfer function is

$$T_{wu}(s) = sT_{\theta u}(s).$$

C. Step response characterization

Global metrics for synchronization performance in e.g. [11], [14], [15], are system norms ($\mathcal{H}_2$, $\mathcal{H}_\infty$) applied to T_{wu} (frequency output), or to a "phase coherency" output based on differences in output angles. The choice of metric carries an implicit assumption on the power disturbances considered (white noise, or a worst-case $\mathcal{L}_2$ signal).

In this paper, we wish to bring metrics closer to industry practice, by considering a *step* input disturbance (e.g. due a fault), and analyzing the response of the vector of bus frequencies $w_i(t)$. Practitioners are interested in some time-domain performance metrics (Nadir, RoCoF, see below) for the response, but transient frequency is bus-dependent.

A candidate global notion of *system frequency* is the weighted average $\bar{w}(t)$ in (1). We now show that for our family of heterogenous systems, the behavior of $\bar{w}(t)$ decouples nicely from the individual bus deviations $w_i(t) - \bar{w}(t)$, opening the door for a separate analysis of both aspects.

Our input will be a step function $u(t) = u_0 \mathbb{1}_{t \geq 0}$; here u_0 is a given vector direction. In Laplace transforms:

$$w(s) = T_{wu}(s)\frac{1}{s}u_0 = F^{-\frac{1}{2}}VH(s)V^T F^{-\frac{1}{2}}u_0. \tag{8}$$

We now isolate the dynamics corresponding to the eigenvalue $\lambda_0 = 0$ and its eigenvector v_0 from the rest:

$$w(s) = F^{-\frac{1}{2}}v_0 h_0(s)v_0^T F^{-\frac{1}{2}}u_0 + F^{-\frac{1}{2}}V_\perp \tilde{H}(s)V_\perp^T F^{-\frac{1}{2}}u_0;$$

here $\tilde{H}(s) = \mathrm{diag}_{k=1,..,n-1}\left(h_k(s)\right)$.

Noting that $F^{-\frac{1}{2}}v_0 = \alpha_F \mathbf{1}$ from (6), and $h_0(s) = g_0(s)$, the first term above is of the form $\bar{w}(s)\mathbf{1}$, where

$$\bar{w}(s) := \alpha_F^2 \mathbf{1}^T u_0 g_0(s) = \frac{\sum_i u_{0i}}{\sum_i f_i} g_0(s). \qquad (9)$$

The second term will be denoted by $\tilde{w}(s)$; by Assumption 2 it has left half-plane poles. So we have obtained the decomposition

$$w(t) = \bar{w}(t)\mathbf{1} + \tilde{w}(t), \qquad (10)$$

intepreted as follows:

- $\bar{w}(t)$ is a *system frequency* term, applied to all nodes;
- the transient term $\tilde{w}(t)$ represents the individual node deviations from the synchronous response.

D. System frequency

We can obtain more information on the system frequency by observing that since $\mathbf{1}^T F^{\frac{1}{2}} V_\perp = \alpha_F^{-1} v_0^T V_\perp = 0$, we have

$$(\mathbf{1}^T F) \underbrace{F^{-\frac{1}{2}} V_\perp \tilde{H}(s) V_\perp^T F^{-\frac{1}{2}} u_0}_{\tilde{w}(s)} \equiv 0.$$

Therefore $\mathbf{1}^T F w(t) = \bar{w}(t)\mathbf{1}^T F\mathbf{1}$ by (10), which gives

$$\bar{w}(t) = \frac{\sum_i f_i w_i(t)}{\sum_i f_i};$$

the system frequency is a weighted mean of bus frequencies, in proportion to their rating. Noting that $m_i = m f_i$, it follows that $\bar{w}(t)$ is exactly the COI frequency from (1).

Also, returning to (9) we have

$$\bar{w}(t) = \frac{\sum_i u_{0i}}{\sum_i f_i} g_0(t). \qquad (11)$$

Recall that $g_0(t)$ is the angle impulse response of the representative machine, or equivalently its angular frequency step response. Thus $\bar{w}(t)$ corresponds to the frequency observed when exciting the representative machine (in open loop) with the total system disturbance normalized by the total scale.

Remark 1: Note that this result is *independent of L*, i.e. the electrical network does not affect the time response of the system frequency, only the machine ratings themselves. Thus, when the network dependent term ($\tilde{w}$) converges fast to zero, (11) is a natural candidate for a reduced order model similar to the ones recently considered in [21], [22].

In the following sections we analyze its behavior for the previously discussed examples.

E. Quantifying the deviation from synchrony

We now turn our attention to the term $\tilde{w}(t)$ which represents individual bus deviations from a synchronous response. A natural way of quantifying the size of this transient term is through the $\mathcal{L}_2$ norm

$$\|\tilde{w}\|_2^2 = \int_0^\infty |\tilde{w}(t)|^2 dt.$$

We now show how this norm can be computed in terms of the parameters of the scaled network Laplacian, and the impulse response matrix $\tilde{H}(t) = \mathrm{diag}_{k=1,\dots,n-1}(h_k(t))$,

Laplace inverse of $\tilde{H}(s)$, which encapsulates all information on the machine model.

Proposition 1: $\|\tilde{w}\|_2^2 = z_0^T Y z_0$, where:

- $Y \in \mathbb{R}^{(n-1)\times(n-1)}$ is the matrix with elements

$$y_{kl} = \gamma_{kl}\langle h_k, h_l\rangle = \gamma_{kl}\int_0^\infty h_k(t)h_l(t)dt, \qquad (12)$$

$$\text{where } \Gamma = (\gamma_{kl}) := V_\perp^T F^{-1} V_\perp; \qquad (13)$$

- $z_0 := V_\perp^T F^{-\frac{1}{2}} u_0 \in \mathbb{R}^{n-1}$.

Proof: With the introduced notation we have

$$\tilde{w}(t) = F^{-\frac{1}{2}} V_\perp \tilde{H}(t) z_0,$$

therefore $\tilde{w}(t)^T \tilde{w}(t) = z_0^T \tilde{H}(t)\Gamma\tilde{H}(t)z_0$. The matrix in the above quadratic form has elements $h_k(t)\gamma_{kl}h_l(t)$, therefore integration in time yields the result. ∎

Remark 2: The metric $\|\tilde{w}\|_2^2$ *does* depend on the electrical network, through the eigenvalues and eigenvectors of L_F.

F. Mean synchronization cost for random disturbance step

Since the cost discussed above is a function of the disturbance step u_0, it may be useful to find its average over a random choice of this excitation. Recalling that the components u_{0i} correspond to different buses, it is natural to assume them to be independent, and thus $E[u_0 u_0^T] = \Sigma^u$, a diagonal matrix. Therefore

$$E[z_0 z_0^T] = V_\perp^T F^{-1} \Sigma^u V_\perp =: \Sigma^z,$$

and the expectation for the cost in Proposition 1 is

$$E\left[\|\tilde{w}\|_2^2\right] = E[z_0^T Y z_0] = E[\mathrm{Tr}(Y z_0 z_0^T)] = \mathrm{Tr}(Y\Sigma^z).$$

We look at some special cases:

- $\Sigma_u = I$ (uniform disturbances). Then $\Sigma^z = \Gamma$, and

$$E\left[\|\tilde{w}\|_2^2\right] = \mathrm{Tr}(Y\Gamma) = \sum_{k,l} \gamma_{kl}^2 \langle h_k, h_l\rangle.$$

- $\Sigma_u = F$. This means disturbance size follows the square root of the bus rating. Here $\Sigma^z = I$, and

$$E\left[\|\tilde{w}\|_2^2\right] = \mathrm{Tr}(Y) = \sum_k \gamma_{kk}\|h_k\|_2^2.$$

- $\Sigma_u = F^2$. This is probably most natural, with disturbances proportional to bus rating. Here $\Sigma^z = V_\perp^T F V_\perp = \Gamma^\dagger$ (pseudoinverse); $E\left[\|\tilde{w}\|_2^2\right] = \mathrm{Tr}(Y\Gamma^\dagger)$.

G. The homogeneous case

If all machines have the same response $g_0(s)$, setting $F = I$ we can obtain some simplifications:

- $\{\lambda_k\}$ are the eigenvalues of the original Laplacian L.
- The system frequency is the average $\bar{w}(t) = \frac{1}{n}\sum_i w_i(t)$, and satisfies

$$\bar{w}(t) = \frac{1}{n}\left(\sum_i u_{0i}\right)g_0(t).$$

- $z_0 = V_\perp^T u_0$, and $\Gamma = V_\perp^T V_\perp = I$. Therefore the matrix Y in Proposition 1 is diagonal, $Y = \mathrm{diag}(\|h_k\|^2)$, and

$$\|\tilde{w}\|_2^2 = \sum_{k=1}^{n-1}(z_{0k})^2\|h_k\|^2, \qquad (14)$$

where $z_{0k} = v_k^T u_0$ is the projection of the excitation vector u_0 in the direction of the k-th eigenvector of the Laplacian L.

- The mean synchronization cost for $E[u_0 u_0^T] = I$ (here all the preceding cases coincide) is

$$E\left[\|\tilde{w}\|_2^2\right] = \sum_{k=1}^{n-1} \|h_k\|_2^2 = \|\tilde{H}\|_{\mathcal{H}_2}^2, \quad (15)$$

the $\mathcal{H}_2$ norm of the transfer function $\tilde{H}(s)$. We recall that this was obtained by isolating the portion $g_0(s)$ corresponding to the synchronized response (in this case, projecting onto $\mathbf{1}^\perp$). In this form, the cost resembles other proposals [11], [15], for the price of synchrony, and [16] for the evaluation of the synchronization cost under step changes in homogeneous systems.

III. APPLICATION TO THE SWING DYNAMICS

In this section we assume we are in the situation of Example 1, i.e., the representative machine is

$$g_0(s) = \frac{1}{s(ms+d)}.$$

and $m_i = f_i m$, $d_i = f_i d$ are the individual bus parameters. The corresponding closed loop transfer functions in (7) are

$$h_k(s) = \frac{1}{ms^2 + ds + \lambda_k}, \quad k = 0, 1, \dots, n-1. \quad (16)$$

Note they are stable when $\lambda_k > 0$.

A. System frequency

Inverting the transform and invoking (11) we find that

$$\bar{w}(t) = \frac{\sum_i u_{0i}}{\sum_i f_i} \overbrace{\frac{1}{d}\left(1 - e^{-\frac{d}{m}t}\right)}^{g_0(t)} \quad (17)$$

$$= \frac{\sum_i u_{0i}}{\sum_i d_i}\left(1 - e^{-\frac{d}{m}t}\right), \quad t > 0. \quad (18)$$

Some comments are in order:

- Again, we recall $\bar{w}(t)$ does not depend on the electrical network.
- The first-order evolution of $\bar{w}(t)$ implies there is no overshoot; system frequency never deviates to a "Nadir" further from equilibrium than its steady-state value.
- The asymptotic frequency $w_\infty = \frac{\sum_i u_{0i}}{\sum_i d_i}$ is the ratio of total disturbance to total damping, but does not depend on the inertia m. The latter only affects the time constant in which this asymptote is achieved.
- The maximum RoCoF (rate-of-change-of frequency) occurs at $t \to 0+$, and is given by

$$\frac{d}{m}\frac{\sum_i u_{0i}}{\sum_i d_i} = \frac{\sum_i u_{0i}}{\sum_i m_i}; \quad (19)$$

here the total inertia appears, which is natural in a second-order response to a step in forcing. RoCoF increases for low inertia, however it need not have a detrimental impact: system frequency initially varies quickly but never deviates more than w_∞, independent of m.

B. Synchronization cost

We now turn to the synchronization cost $\|\tilde{w}\|_2$, which can be computed by particularizing the result in Proposition 1. The following result is proved in Appendix I.

Proposition 2: Let $h_k(s)$ be given in (16), and $h_k(t)$ its inverse transform, for $k = 1, \dots, n-1$. Then:

$$\langle h_k, h_l \rangle = \frac{2d}{m(\lambda_k - \lambda_l)^2 + 2(\lambda_k + \lambda_l)d^2}. \quad (20)$$

It follows that the matrix Y in (12) will depend on both inertia m and damping d, so in general both have an impact on the "price of synchrony". Note however that inertia only appears in off-diagonal terms, and the matrix remains bounded as $m \to 0$ or $m \to \infty$; we thus argue that inertia has limited impact. We look at this issue in further detail.

1) Homogeneous case: In the case of homogeneous machines, we saw above that $\Gamma = I$ and Y is diagonal, so inertia disappears completely: indeed using (14) we have

$$\|\tilde{w}\|_2^2 = \sum_{k=1}^{n-1} \frac{(v_k^T u_0)^2}{2d\lambda_k}. \quad (21)$$

The cost is inversely proportional to damping, and the direction of the disturbance u_0 also matters. Recalling that v_k is the k-th Laplacian eigenvector, the worst-case for a given magnitude $|u_0|$ is when it is aligned to v_1, the Fiedler eigenvector.

If the disturbance direction is chosen randomly as in Section II-G, then (15) gives

$$E\left[\|\tilde{w}\|_2^2\right] = \sum_k \|h_k\|_2^2 = \frac{1}{2d}\sum_k \frac{1}{\lambda_k} = \frac{1}{2d}\text{Tr}(L^\dagger); \quad (22)$$

again a similar result to those in [11] for homogeneous systems.

2) Heterogeneous, high inertia case: Assume for this discussion that all the λ_k are distinct; then as $m \to \infty$ we have $y_{kl} \to 0$ for $k \neq l$, so Y again becomes diagonal, and the cost has the limiting expression

$$\|\tilde{w}\|_2^2 \xrightarrow{m\to\infty} \sum_{k=1}^{n-1} \frac{\gamma_{kk} z_{0k}^2}{2d\lambda_k}. \quad (23)$$

So the high inertia behavior is of a similar structure to the homogeneous case in (21). Comparisons are not straightforward, though, since the scaling factor F affects z_{0k}, γ_{kk} and λ_k in each of the above terms.

3) Heterogeneous, low inertia case: If $m \to 0$, then the limiting Y matrix is not diagonal. The corresponding limiting cost is

$$\|\tilde{w}\|_2^2 \xrightarrow{m\to0+} \sum_{k,l=1}^{n-1} \frac{\gamma_{kl} z_{0k} z_{0l}}{d(\lambda_k + \lambda_l)}. \quad (24)$$

Note, however, that the diagonal terms are the same as in the high inertia case. This suggests that inertia plays a limited role in the $\mathcal{L}_2$ price of synchrony, even in the heterogeneous machine case.

IV. MODEL WITH TURBINE DYNAMICS

We now turn to the model of Example 2, where the representative machine is

$$g_0(s) = \frac{\tau s + 1}{s\left(m\tau s^2 + (m + d\tau)s + d + r^{-1}\right)}. \quad (25)$$

The corresponding closed loop transfer functions in (7) for $k = 0, 1, \ldots, n - 1$ are:

$$h_k(s) = \frac{\tau s + 1}{m\tau s^3 + (m + d\tau)s^2 + (d + r^{-1} + \lambda_k \tau)s + \lambda_k}. \quad (26)$$

It can be checked (e.g. by applying the Routh-Hurwitz criterion) that $h_k(s)$ is stable whenever $\lambda_k > 0$.

A. System frequency

We can again use (11) and (25) to compute the system frequency

$$\bar{w}(t) = \frac{\sum_i u_{0i}}{\sum_i f_i} \mathcal{L}^{-1}\{g_0(s)\}, \quad (27)$$

but now the inverse transform of $g_0(s)$ is more involved.

Using partial fractions we first express

$$g_0(s) = \frac{1}{d + r^{-1}}\left(\frac{1}{s} - \frac{s + \left(\frac{1}{\tau} - \frac{r^{-1}}{m}\right)}{s^2 + \left(\frac{1}{\tau} + \frac{d}{m}\right)s + \frac{d + r^{-1}}{m\tau}}\right)$$

The first term provides the steady-state response, which is

$$w_\infty = \frac{\sum_i u_{0i}}{\sum_i f_i}\frac{1}{d + r^{-1}} = \frac{\sum_i u_{0i}}{d_i + r_i^{-1}};$$

this is analogous to the swing equation case, except than the droop control has been added to the damping. Again, we observe that inertia plays no role at all in this steady-state deviation.

The transient term is a second-order transfer function, which we proceed to analyze now. Its behavior critically depends on whether its poles are real or complex conjugate. In particular, whenever

$$\frac{d + r^{-1}}{m\tau} - \frac{1}{4}\left(\frac{1}{\tau} + \frac{d}{m}\right)^2 =: \omega_d^2 > 0 \quad (28)$$

the system is under-damped with poles $\eta \pm j\omega_d$, and

$$g_0(t) = \mathcal{L}^{-1}\left\{\frac{1}{d + r^{-1}}\left(\frac{1}{s} - \frac{s + \gamma}{(s + \eta)^2 + \omega_d^2}\right)\right\}$$

$$= \frac{1}{d + r^{-1}}\left[1 - e^{-\eta t}\left(\cos(\omega_d t) - \frac{(\gamma - \eta)}{\omega_d}\sin(\omega_d t)\right)\right] \quad (29)$$

where

$$\eta := \frac{1}{2}\left(\frac{1}{\tau} + \frac{d}{m}\right) \quad \text{and} \quad \gamma := \left(\frac{1}{\tau} - \frac{r^{-1}}{m}\right). \quad (30)$$

The system frequency time evolution is given by

$$\bar{w}(t) = \frac{\sum_i u_{0i}}{\sum_i d_i + r_i^{-1}}g_0(t), \quad (31)$$

with $g_0(t)$ from (29).

A few observations are in order:

- Including the turbine model has a nontrivial effect on the system frequency $\bar{w}(t)$. It is the presence of the turbine dynamics that provides the characteristic under-damped behavior that produces a Nadir.
- We have only provided here the solution of $\bar{w}(t)$ for the (practically more relevant) under-damped case.
- Interestingly, (28) shows that the system may become over-damped by either increasing m, or decreasing m! However, the behavior is different for each case: in the very high inertia case the Nadir disappears; whereas when m goes to zero, there is an overshoot in the overdamped response. Since in practice this occurs only for very low inertia and already way beyond the acceptable deviation, we are justified in our focus on the under-damped case.

We now proceed to compute the Nadir and RoCoF for this situation.

1) Nadir:
In order to compute the Nadir we will use

$$||\bar{w}||_\infty = \left|\frac{\sum_i u_{0i}}{\sum_i f_i}\right|||g_0||_\infty.$$

Thus, one can compute the Nadir by finding the maximum excursion of $g_0(t)$. The following proposition summarizes the overall calculation.

Proposition 3 (Nadir): Given a power system under Assumption 1 with generators containing first order turbine dynamics ($g_i(s)$ given by (3)). Then under the under-damped condition (28), the Nadir is given by

$$||\bar{w}||_\infty = \frac{|\sum_i u_{0i}|}{\sum_i f_i}\frac{1}{d + r^{-1}}\left(1 + \sqrt{\frac{\tau r^{-1}}{m}}e^{-\frac{\eta}{\omega_d}\left(\phi + \frac{\pi}{2}\right)}\right), \quad (32)$$

where the phase $\phi \in (-\frac{\pi}{2}, \frac{\pi}{2})$ is uniquely determined by

$$\sin(\phi) = \frac{\left(\frac{1}{\tau} - \eta\right)}{\sqrt{\omega_d^2 + \left(\frac{1}{\tau} - \eta\right)^2}} = \frac{m - d\tau}{2\sqrt{m\tau r^{-1}}}. \quad (33)$$

The dependence of (32) on m is not straightforward, as ϕ, η, and ω_d depend on it. The next proposition shows that the dependence is as expected by conventional power engineering wisdom.

Proposition 4: Given a power system under Assumption 1 with generators containing first order turbine dynamics ($g_i(s)$ given by (3)). Then under the under-damped condition (28), the maximum frequency deviation $||\bar{w}||_\infty$ is a decreasing function of m, i.e., $\frac{\partial}{\partial m}||\bar{w}||_\infty < 0$.

The proof is referred to [23] due to space limitations.

2) RoCoF:
A similar procedure as the one used to study the Nadir of the system frequency can be used to investigate the properties of the maximum rate of change of frequency (RoCoF).

Proposition 5 (RoCoF): Given a power system under Assumption 1 with generators containing first order turbine dynamics ($g_i(s)$ given by (3)). Then under the under-damped condition (28), the RoCoF is given by

$$||\dot{\bar{w}}||_\infty = \frac{|\sum_i u_{0,i}|}{\sum_i f_i}\frac{1}{m}. \quad (34)$$

The proof of Proposition 5 can also be found in [23]; the main difference with Proposition 3 is that, while not trivial to establish, here the maximum is always achieved at $t = 0+$, exactly as in the second order case of (19).

The dependence of $\|\dot{w}\|_\infty$ on m is now easily addressed and again as expected: RoCoF decreases with m.

B. Synchronization cost

The synchronization cost $\|\tilde{w}\|^2$ can once again be computed through Proposition 1, which requires finding the inner products $\langle h_k, h_l \rangle$, in this case for the functions in (26).

Since the corresponding expression is in general rather unwieldy (see [23]), we will present some simpler cases, beginning with $k = l$; the norm, found in Appendix I is:

$$\|h_k\|_2^2 = \frac{m + \tau(\lambda_k \tau + d)}{2\lambda_k \left[m(r^{-1} + d) + \tau d(r^{-1} + \lambda_k \tau + d) \right]}. \quad (35)$$

1) Homogeneous case: The above expression suffices to analyze the case of homogeneous machines, where $\Gamma = I$ and Y is diagonal. We have from (14) that

$$\|\tilde{w}\|_2^2 = \sum_{k=1}^{n-1} (v_k^T u_0)^2 \|h_k\|_2^2;$$

from (35) we see that, in contrast to the second order machine model, the inertia m does affect the synchronization cost. A closer look at $\|h_k\|^2$ as a (linear fractional) function of m shows that it is *decreasing* in $m \in (0, \infty)$, going from

$$\|h_k\|_2^2 \xrightarrow{m \to 0+} \frac{1}{2\lambda_k d} \cdot \frac{\lambda_k \tau + d}{r^{-1} + \lambda_k \tau + d},$$

to

$$\|h_k\|_2^2 \xrightarrow{m \to \infty} \frac{1}{2\lambda_k d} \cdot \frac{d}{r^{-1} + d}.$$

So higher inertia is beneficial in this case. Recalling that the corresponding cost for the swing dynamics is $\frac{1}{2\lambda_k d}$, we see that this cost has been reduced. In the high inertia case, the main change is the increased damping through the droop coefficient r^{-1}.

2) Heterogeneous, high inertia case: As mentioned, the formula for $\langle h_k, h_l \rangle$ for $k \neq l$ is quite formidable, but we can give its approximation in the limit of large m:

$$\langle h_k, h_l \rangle \overset{m \to \infty}{\sim} \frac{2(d + r^{-1})}{m(\lambda_k - \lambda_l)^2}, \quad k \neq l.$$

This assumes $\lambda_k \neq \lambda_l$. So if the eigenvalues of the scaled Laplacian L_F are distinct, we see that again the matrix Y becomes diagonal as $m \to \infty$. The limiting cost is

$$\|\tilde{w}\|_2^2 \overset{m \to \infty}{\longrightarrow} \sum_{k=1}^{n-1} \frac{z_{0k}^2 \gamma_{kk}}{2\lambda_k d} \cdot \frac{d}{r^{-1} + d}.$$

This expression amounts to reducing to the cost (23) for the second order dynamics, by the fraction $\frac{d}{r^{-1}+d}$. So the role of the turbine in a high inertia system is again mainly a change in the droop coefficient.

3) Heterogeneous, low inertia case: In the low inertia limit, we find that $\langle h_k, h_l \rangle \overset{m \to 0}{\longrightarrow} \frac{N}{D}$, where

$$N = 2d(d + r^{-1}) + \tau(2d + r^{-1})(\lambda_k + \lambda_l) + 2\lambda_k \lambda_l \tau^2,$$
$$D = 2d(d + r^{-1})^2(\lambda_k + \lambda_l) + d\tau(2d + r^{-1})(\lambda_k + \lambda_l)^2$$
$$+ 2d\tau\lambda_k\lambda_l[2r^{-1} + \tau(\lambda_k + \lambda_l)].$$

So the limiting matrix Y is not diagonal, as in the second order case; an expression analogous to (24) can be written. Comparisons between the two are not straightforward here, and must be pursued by numerical experimentation.

V. CONCLUSIONS

We have studied system-theoretic measures of synchronization performance, with the aim of covering more realistic scenarios than the recent literature, and also closing the gap with power engineering practice. In particular, for a family of heterogeneous machine systems, we have focused on the step response of the bus frequency vector, decomposed as a system-wide weighted mean and the vector of relative differences to it. The key mathematical assumption is a relative proportionality in machine parameters, which may be incorporated together with the network model to perform an adequate diagonalization.

With this transformation, the natural system frequency (motion of the COI) becomes independent of the network, and its characteristics can be studied through a representative machine. The energy of the synchronization error around this mean depends on both network and machine models, but we have an expression that encapsulates the latter in terms of a matrix of inner products. From this general result special cases can be studied.

A key question of interest to practitioners is the role of inertia, in particular whether low inertia can compromise performance. Our analysis shows that if a second-order, swing equation model is used for each machine, the impact of inertia is small. The global system frequency exhibits no overshoot, inertia affecting mainly its time constant; while inertia appears in the energy of oscillations, its impact is not significant. The story changes if a dynamic model of turbine control is adopted, where the turbine time-constant is in the order of magnitude of the swing dynamics. In that case, inertia does play a positive role, providing resilience of the peak system frequency deviation and reducing the norm of relative oscillations.

Future work will involve carrying out these calculations for actual networks with real parameters.

APPENDIX I
INNER PRODUCT COMPUTATION

We show here how to evaluate the inner product in (12) using state-space methods. We start with a state-space realization of the representative machine,

$$g_0(s) = \left[\begin{array}{c|c} A & B \\ \hline C & 0 \end{array} \right].$$

If follows easily that each h_k in (7) has realization

$$h_k(s) = \left[\begin{array}{c|c} A_k & B \\ \hline C & 0 \end{array} \right], \quad \text{where } A_k = A - \lambda_k BC.$$

Note that the state matrix A_k is the only one that depends on the eigenvalue λ_k under consideration. By Assumption 2, A_k is a Hurwitz matrix for any $\lambda_k > 0$.

Writing $h_k(t) = Ce^{A_k t}B$ for the impulse response, we compute the inner product between two such functions:

$$
\begin{aligned}
\langle h_k, h_l \rangle &= \int_0^\infty h_k(t) h_l(t)^T dt \\
&= C \underbrace{\left(\int_0^\infty e^{A_k t} BB^T e^{A_l^T t} dt \right)}_{Q_{kl}} C^T;
\end{aligned}
\tag{36}
$$

here ^{T} denotes matrix transpose. A standard calculation shows that Q_{kl} satisfies the Sylvester equation

$$
A_k Q_{kl} + Q_{kl} A_l^T + BB^T = 0. \tag{37}
$$

Furthermore since the eigenvalues of A_k, A_l never add up to zero it follows (see [24]) that (37) has a unique solution Q_{kl}. Thus, the relevant inner product can be found by solving the above linear equation and substituting into (36).

Second order machine model

In the situation of Section III, it is easily checked that

$$
A_k = \begin{bmatrix} 0 & 1 \\ -\frac{\lambda_k}{m} & -\frac{d}{m} \end{bmatrix} \quad B = \begin{bmatrix} 0 \\ -\frac{1}{m} \end{bmatrix}; \quad C = \begin{bmatrix} 1 & 0 \end{bmatrix}.
$$

In this case the solution to the Sylvester equation is

$$
Q_{kl} = \frac{2d}{m(\lambda_k - \lambda_l)^2 + 2(\lambda_k + \lambda_l)d^2} \begin{bmatrix} 1 & \frac{\lambda_k - \lambda_l}{2d} \\ \frac{\lambda_l - \lambda_k}{2d} & \frac{\lambda_k + \lambda_l}{2m} \end{bmatrix};
$$

Substitution into (36) for the given C proves Proposition 2.

Third order machine model, $k = l$

Here the relevant matrices are

$$
A_k = \begin{bmatrix} 0 & 1 & 0 \\ -\frac{\lambda_k}{m} & -\frac{d}{m} & \frac{1}{m} \\ 0 & -\frac{r^{-1}}{\tau} & -\frac{1}{\tau} \end{bmatrix}; \; B = \begin{bmatrix} 0 \\ -\frac{1}{m} \\ 0 \end{bmatrix}; \; C = \begin{bmatrix} 1 & 0 & 0 \end{bmatrix}.
$$

The Sylvester equations for Q_{kl} in this case (9 linear equations, 9 unknowns) give unwieldy expressions which are not practical to include here. The limiting cases of $m \to 0$ and $m \to \infty$ were presented in Section IV.

What remains tractable is the case $k = l$; here we have a Lyapunov equation with symmetric solution

$$
Q_{kk} = \frac{1}{\Delta} \begin{bmatrix} \frac{m + \tau(\lambda_k + d)}{\lambda_k} & 0 & -\tau r^{-1} \\ 0 & \frac{m + \tau(r^{-1} + \lambda_k \tau + d)}{m} & -r^{-1} \\ -\tau r^{-1} & r^{-1} & r^{-2} \end{bmatrix},
\tag{38}
$$

where $\Delta = 2[m(r^{-1} + d) + \tau d(r^{-1} + d + \lambda_k \tau)]$. By looking at the $(1,1)$ element of this matrix we find the norm $\|h_k\|^2 = \langle h_k, h_k \rangle$, which coincides with the expression given in (35).

REFERENCES

[1] R. D. Evans and R. C. Bergvall, "Experimental analysis of stability and power limitations," *Journal of the A.I.E.E.*, vol. 43, no. 4, pp. 329–340, Apr. 1924.

[2] C. P. Steinmetz, "Power control and stability of electric generating stations," *Journal of the A.I.E.E.*, vol. 39, no. 2, pp. 1215–1287, July 1920.

[3] North American Electric Reliability Corporation, "2015 Frequency Response Annual Analysis," Tech. Rep., Sept. 2015.

[4] Federal Energy Regulatory Commission and North American Electric Reliability Corporation, "Arizona-Southern California Outages on September 8, 2011," Tech. Rep., Apr. 2012.

[5] Y.-Y. Hsu, S.-W. Shyue, and C.-C. Su, "Low frequency oscillations in longitudinal power systems: Experience with dynamic stability of Taiwan power system," *IEEE Trans. on Power Systems*, vol. 2, no. 1, pp. 92–98, Feb. 1987.

[6] M. Klein, G. J. Rogers, and P. Kundur, "A fundamental study of inter-area oscillations in power systems," *IEEE Trans. on Power Systems*, vol. 6, no. 3, pp. 914–921, 1991.

[7] M. M. Begovic, "Inter-area oscillations in power systems: A nonlinear and nonstationary perspective (messina, a.r.) [book reviews]," *IEEE Power and Energy Magazine*, vol. 9, no. 2, pp. 76–77, 2011.

[8] N. W. Miller, M. Shao, and S. Venkataraman, "California ISO (CAISO) Frequency Response Study ," General Electric, Tech. Rep., Nov. 2011.

[9] J. Winkelman, J. Chow, B. Bowler, B. Avramovic, and P. Kokotovic, "An analysis of interarea dynamics of multi-machine systems," *IEEE Transactions on Power Apparatus and Systems*, vol. PAS-100, no. 2, pp. 754–763, 1981.

[10] G. Verghese, I. Pérez-Arriaga, and F. Schewppe, "Selective modal analysis with applications to electric power systems, part ii: the dynamic stability problem," *IEEE Transactions on Power Apparatus and Systems*, vol. PAS-101, no. 9, pp. 3126–3134, 1982.

[11] E. Tegling, B. Bamieh, and D. Gayme, "The price of synchrony: Evaluating the resistive losses in synchronizing power networks," *IEEE Transactions on Control of Network Systems*, vol. 2, no. 3, pp. 254–266, 2015.

[12] A. Mešanović, U. Münz, and C. Heyde, "Comparison of $\mathcal{H}_\infty$, $\mathcal{H}_2$, and pole optimization for power system oscillation damping with remote renewable generation," *IFAC-PapersOnLine*, vol. 49, no. 27, pp. 103–108, 2016.

[13] E. Mallada, "iDroop: A dynamic droop controller to decouple power grid's steady-state and dynamic performance," in *55th IEEE Conference on Decision and Control (CDC)*, 12 2016, pp. 4957–4964.

[14] B. K. Poolla, S. Bolognani, and F. Dorfler, "Optimal placement of virtual inertia in power grids," *IEEE Transactions on Automatic Control*, 2017.

[15] M. Pirani, J. W. Simpson-Porco, and B. Fidan, "System-Theoretic Performance Metrics for Low-Inertia Stability of Power Networks," *ArXiv e-prints*, Mar. 2017.

[16] M. Andreasson, E. Tegling, H. Sandberg, and K. H. Johansson, "Coherence in Synchronizing Power Networks with Distributed Integral Control," *ArXiv e-prints*, Mar. 2017.

[17] Y. Jiang, R. Pates, and E. Mallada, "Performance tradeoffs of dynamically controlled grid-connected inverters in low inertia power systems," in *56th IEEE Conference on Decision and Control (CDC)*, 2017.

[18] P. Kundur, *Power System Stability and Control*. McGraw-Hill Professional, 1994.

[19] A. Bergen and V. Vittal, *Power System Analsysis*. Prentice-Hall, 2000.

[20] G. Kou, S. W. Hadley, P. Markham, and Y. Liu, "Developing Generic Dynamic Models for the 2030 Eastern Interconnection Grid," Oak Ridge National Laboratory, Tech. Rep., Dec 2013. [Online]. Available: http://www.osti.gov/scitech/

[21] S. S. Guggilam, C. Zhao, E. Dall'Anese, Y. C. Chen, and S. V. Dhople, "Engineering inertial and primary-frequency response for distributed energy resources," *arXiv preprint arXiv:1706.03612*, 2017.

[22] D. Apostolopoulou, P. W. Sauer, and A. D. Domínguez-García, "Balancing authority area model and its application to the design of adaptive agc systems," *IEEE Transactions on Power Systems*, vol. 31, no. 5, pp. 3756–3764, 2016.

[23] F. Paganini and E. Mallada, "Global performance metrics for synchronization of heterogeneously rated power systems: The role of machine models and inertia," *Extended version, in preparation for arXiv*, 2017.

[24] K. Zhou, J. Doyle, and K. Glover, *Robust and Optimal Control*. Prentice Hall, 1996.